Chinese Chemical Letters 31 (2020) 1665–1669

Contents lists available at ScienceDirect

Chinese Chemical Letters

journal homepage: www.elsevier.com/locate/cclet

Communication

Water permeability in MXene membranes: Process matters

Hang Zhou[a], Yuwei Wang[b], Fuqiang Wang[a], Hao Deng[a], Yongchen Song[a], Changping Li[b,*], Zheng Ling[a,*]

[a] Key Laboratory of Ocean Energy Utilization and Energy Conservation of Ministry of Education, School of Energy & Power Engineering, Dalian University of Technology, Dalian 116024, China
[b] Research Center for Eco-Environmental Engineering, Dongguan University of Technology, Dongguan 523808, China

ARTICLE INFO

Article history:
Received 8 October 2019
Received in revised form 26 October 2019
Accepted 29 October 2019
Available online 2 November 2019

Keywords:
Exfoliation
MXene
Two-dimensional materials
Water permeability
Water treatment

ABSTRACT

Recent studies have shown impressive transport behaviors of water and ions within lamellar MXene membranes, which endows great promise in developing advanced separation application based high performance MXene membranes. However, most of the researches focused on modification of MXene nanoflakes and optimizing interlayer distance, leaving the impact of membrane fabrication process marginal. In this work, we studied the water flux of membranes made by vacuum filtration using delaminated MXene nanoflakes as the building-blocks. Our results show that the water permeability is extremely sensitive to the process, especially at the drying process, loading and deposit rate of nanoflakes (the feeding concentration). We find that the voids from less ordered stack rather than in-plane defects and interlayer galleries contribute to the large water permeability. The voids can be effectively avoided *via* deposition of MXene nanoflakes at a slow rate. Manipulating the stack of MXene nanoflakes during vacuum filtration and drying are critical for development of MXene membranes with desired performance for water permeation.
© 2019 Chinese Chemical Society and Institute of Materia Medica, Chinese Academy of Medical Sciences. Published by Elsevier B.V. All rights reserved.

The state-of-the-art studies on the two-dimensional (2D) materials assembled membranes have stimulated expanding interest in various applications, such as water purification, energy storage and electro-photonics devices [1–8]. The performance of the 2D materials based membranes depends on the properties of 2D materials as the building-blocks and the structure of the assembled membranes [4,9,10].

Graphene is one of the most popular 2D materials for assembling membranes. However, the pristine graphene is hydrophobic, which would limit its processing and direct application in water treatment [11]. So graphene derivates, such as graphene oxides and analogues, have attracted extensive interest worldwide. MXene, a new family of 2D materials composed of transition metal carbides and nitrides [12,13], has shown promising for constructing advanced membrane for water treatment and energy storage due to its hydrophilic properties and excellent electrical conductivity [14,15]. MXenes are commonly synthesized by selectively etching of MAX phases which are ternary carbides and nitrides with a large material pool [12,16]. The synthesis process introduces oxygen-containing groups, leading to hydrophilic charged MXene surfaces [12]. Surface charge and hydrophilicity insure the stability of delaminated MXenes (d-MXene) dispersed in aqueous colloidal solutions with a large range of concentration [17]. This makes the processing of d-MXene easy, particularly for making coating and assembling membranes.

Vacuum filtration is one of the most common ways to fabricate membranes using d-MXene colloidal suspensions [18]. The unprecedented architectures assembled from d-MXene nanoflakes and outstanding properties have attracted extensive attention for water treatment [14,19,20]. Large water permeability through pores in advanced membrane is highly desired for the next generation of water treatment technologies [2]. Therefore, further optimization of MXene based membranes requires high levels of permeate water flux (or permeability) and salt rejection. However, most of the recent researches have focused on modification of MXene nanoflakes and optimizing interlayer distance [14,21], leaving the impact of membrane fabrication process marginal. Understanding the impact of process (such as loading, concentration of feeding or filtration rate) in the structure and the performance of produced membranes is mandatory to rationally design and fully control the performance of the fabricated materials. A profound understanding of what occurs during the assembly and subsequent drying and utilization is required to practically utilize this promising materials. However, there is little work by far.

* Corresponding authors.
E-mail addresses: licpbit@hotmail.com (C. Li), zling@dlut.edu.cn (Z. Ling).

https://doi.org/10.1016/j.cclet.2019.10.037
1001-8417/© 2019 Chinese Chemical Society and Institute of Materia Medica, Chinese Academy of Medical Sciences. Published by Elsevier B.V. All rights reserved.

In this study, we focused on water permeability of the d-MXene membranes since it plays a critical role in water treatment efficiency while the selectivity can be finely turned *via* modification of the d-MXene nanoflakes as the building-blocks [20] or utilization of external assistance, such as electric field [22]. We used $Ti_3C_2T_x$ (where T stands for surface groups, x stands for their contents), the most studied MXene, to explore the process-structure-performance relationship of d-MXene membranes assembled by vacuum filtration. Membranes with different loading were made, their drying-dependent water permeability and structures were studied. The membranes with identical loading were made using different filtration rate and oxidation treatment. Their treat-dependent performance indicates the voids plays the critical role for water flux and can be control *via* proper processing process. This study offers insight for the process-structure-performance relationship of d-MXene membranes, which is useful for making desired membranes assembled from d-MXene.

Materials: High-purity Ti_3AlC_2 MAX phase powders (500 mesh) were purchased from Laizhou Kai Kai Ceramic Materials Co., Ltd. LiF was bought from Alfa Aesar (China) Chemicals Co., Ltd. HCl was purchased from Sinopharm Chemical Reagent Co., Ltd. All the chemical agents were used as-received.

Selectively etching: LiF (1.32 g) was dissolved in 20 mL of 6 mol/L HCl. Ti_3AlC_2 powders were slowly added into the LiF contained acid and the mixture was magnetically stirred at 45 °C for 72 h. The produced sediment was washed 6 times using deionized water till the pH reached 6.5∼7. The sediment (multi-layer MXene, Ml-MXene) was naturally dried for 24 h. The delamination of Ml-MXene was conducted in ice bath for 1 h under flowing N_2. The delaminated MXene (d-MXene) colloidal suspension was obtained after centrifugation at 3500 rpm for 1 h. The concentration of d-MXene suspension was found by our previously reported method [23].

Membrane fabrication: Colloidal suspensions of d-MXene were used to fabricate membranes with anodized alumina (with an average pore size of 20 nm from GE Healthcare company) filter membrane. The loading of d-MXene membranes was controlled *via* the amount of the d-MXene colloidal suspension with definite concentration. The d-MXene membranes with loading of 0.1, 0.3 and 0.5 mg/cm^2 were fabricated using the suspension with a concentration of 0.81 mg/mL.

Characterizations: The morphology was analyzed using scanning electron microscopy (SU8200, 5.0 kV) and transmission electron microscopy (JEOL JEM-2100 F, 200 kV). X-ray diffraction analysis was conducted using a Bruker D8 Advanced with filtered Cu Kα radiation (λ = 0.154 nm, operated at 40 kV and 40 mA). The 2θ range was set from 3° to 10°, with a step 1.5°/min. Raman spectra were acquired using LabRAM HR Evolution, with a 532 nm excitation line and an 1800 lines/mm grating. The contact angles were tested using industrial camera (UI-1220LE-M-GL, developed by IDS-Germany) and SurfaceMeter^{TM} software (developed by Ningbo NB Scientific Instruments Co., Ltd.) with a single drop volume of 8 μL.

Water flux test: Loading- and drying-dependent water flux. The d-MXene membranes with loading of 0.1, 0.3 and 0.5 mg/cm^2 were used for the test. In a typical run, the fresh d-MXene membrane was made *via* vacuum filtration. The membrane was filtrated for extra 10 min after there was no visible water. Then the as-made membrane was naturally dried for 1 h. After drying, 10 mL water was filtrated the pressure and finishing time were recorded for calculating the water flux. The drying dependent performance was studying over 5, 12, 24, 48 and 72 h.

In order to study the impact of deposition rate on the water flux, we used the feeding suspensions with different concentrations, including 0.27 mg/mL and 0.0081 mg/mL, to make d-MXene membranes with identical loading of 0.3 mg/cm^2. The membrane preparation and water flux test used the same processes as above. The naturally drying intervals were 1, 2, 4, 12, 24 and 48 h.

The oxidation was conducted on the d-MXene membrane (0.3 mg/cm^2, feeding concentration of 0.27 mg/mL). In a typical run, the membrane was made using the same process as above. After 10 min drying, 10 mL 0.3 wt% H_2O_2 was filtrated under vacuum, then the membrane was dried for 10 min under vacuum filtration. The oxidized membrane was used for water flux test.

Selectively etching of Al layers from Ti_3AlC_2 is the most common way to synthetize Ml-MXene [15,18]. As shown in Figs. S1a and b (Supporting information), the dense MAX particles were turned into laminates with more distinct multilayers stacking. The Li^+ used in the etching agents spontaneously intercalated into the interlayers of Ml-MXene, facilitating the delamination of Ml-MXene [18]. Stable colloidal suspensions of d-MXene were obtained after centrifugation (Fig. S1c in Supporting information). Single or few-layered d-MXene nanoflakes were produced *via* delamination as shown in Figs. 1a and b and Fig. S2 (Supporting information). Laminar d-MXene membranes were orderly stacked by vacuum filtration (Fig. 1c). The Raman spectra indicated there is not composition change between Ml-MXene and d-MXene membrane (Fig. S3 in Supporting information). The loading (thickness) can be elegantly adjusted by controlling the amount of filtrated d-MXene suspension (Fig. S4 in Supporting information). By stacking d-MXene nanoflakes, laminar d-MXene membranes provide three types channels for water and other molecules or ions transportation, including in-plane nanopores *via* defects, interplane galleries (with slit-like pores formed by inter-edge nanoflake interactions as the entrances of the galleries) and voids from less ordered stack of nanoflakes (Fig. 1d), which are similar with the channels formed in graphene oxides or other 2D material laminate membranes [11,24,25].

The formed channels in stacked d-MXene membranes allow the passage of water and other molecules or ions during water treatment. The d-MXene membranes with loading of 0.1 and 0.3 mg/cm^2 have a relatively constant porosity of around 59% (porosity and thickness can be found in Table S1 in Supporting information), suggesting that identical process in the membrane fabrication produces d-MXene membranes with similar interior structures as shown in the SEM images (Fig. S4). As the loading increased to 0.5 mg/cm^2, the porosity decreased to about 39% due to the compaction caused by stacking more d-MXene nanoflakes.

The mass loading has a negligible impact on the contact angle of the as-made d-MXene membranes, as shown in Fig. 2a. All the membranes share a similar contact angle of around 50°, indicating

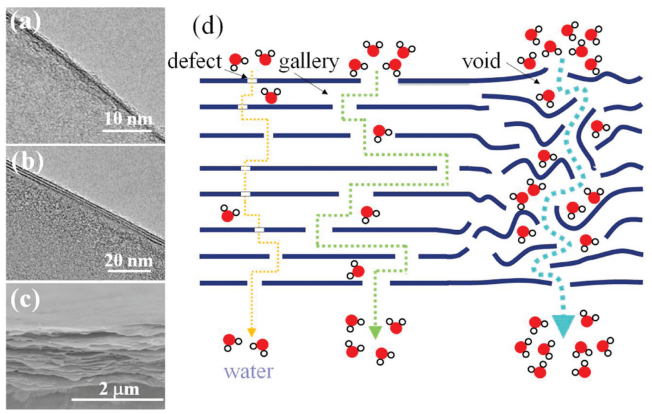

Fig. 1. (a, b) TEM images of single- and few-layered d-MXene nanoflakes. (c) SEM image of the laminar d-MXene membrane with a loading of 0.5 mg/cm^2. (d) schematic diagram of water channels (including defects in the d-MXene nanoflakes, galleries between nanoflakes, and voids from less ordered stack of nanoflakes) in as-made d-MXene membrane.

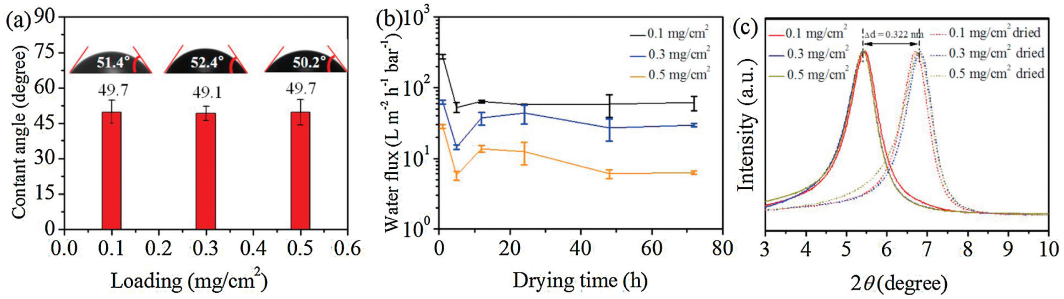

Fig. 2. (a) Contact angles of d-MXene membranes with different loading, (b) water flux of d-MXene membranes after drying for various time. (c) XRD patterns of the d-MXene membranes with different loading. The solid lines stand for the pristine membranes after vacuum filtration, the dash lines stand for the same membranes after naturally drying for 30 h under vacuum.

the hydrophilic feature of MXene. The water flux of the as-made d-MXene membranes are both mass loading- and drying-dependent, as shown in Fig. 2b. The increased mass loading leads to monotonic decrease in water flux, due to the increased thickness and reduced porosity (Table S1) of the membranes with larger loading. The tortuosity and the total length of the channels are greatly enhanced with the increased loading [26], since there are more nanoflakes stacking at the same area. The decrescent porosity was caused by the severe compaction due to build-up of more nanoflakes at a larger loading. The enhanced tortuosity, channel length and compaction lead to the degradation in water flux of d-MXene membranes with larger loading.

The drying-dependent water fluxes are different for the d-MXene membranes with various loadings. All the membranes show dramatic reduction in flux after drying for 1 h, reaching their minimum values. The flux regains at different rate, with the thinnest membrane (smallest loading) having the fastest rate for recovery in its water flux. The drying-dependent water permeability is related to the hydration of the d-MXene membranes. It is well-known that the hydration process and degree have critical impacts on the structure, separation performance and stability of the membranes assembled of 2D materials [1,27,28]. Even worse, uncontrolled hydration, such as dramatic swelling, would damage the structural stability, degrading the performance [27]. Therefore, various methods were proposed to control the hydration degree to obtain membranes with desired performance [11]. During the hydration process, water molecules intercalate the interlayers of nanoflakes. Therefore, the amount of intercalated water determines the interlayer distance as demonstrated in our previous work on the MXene films [29].

Drying is the inverse process of hydration. Water molecules are removed during the drying process, leading to the shrink in the interlayer distance. XRD was used to figure out the impact of water on the interlayer distance of d-MXene membranes. The pristine d-MXene membranes after vacuum filtration, regardless of the loading, have the almost identical interlayer distance as indicated by the XRD peaks locating at 5.4° (corresponding to a distance of 1.626 nm), as shown in Fig. 2c. After drying for 30 h at room temperature under vacuum, all the XRD peaks move to about 6.8°, confirming the shrunk interlayer distances (around 1.304 nm) due to the removal of water. Additionally, both the pristine and dried membranes show intact peaks independent of the loading, indicating that the d-MXene membranes sharing almost identical interior structures. In the dry state, d-MXene membranes with different loading have similar interlayer free spacings (unoccupied space between neighboring d-MXene nanoflakes), which may be responsible for the stabilized water flux after drying for 48 h (Fig. 2b).

Like the molecular transport through graphene oxide laminates [11], water transport through d-MXene membranes occurs in in-plane defects and slit-like pores, and then in interlayer galleries during the water flux test. The in-plane defects should be similar, since the nanoflakes are identical. The XRD indicates similar interior gallery structures. However, the inconsistent water flux change suggests that there are other factor rather than defects and galleries determining the water flux. Voids from less ordered stack of nanoflakes is confirmed to be responsible for the abnormally large water flux of films assembled of 2D material [24]. We believe voids also play the critical role in our d-MXene membranes.

The practical performance is highly dependent on the uniform of the membranes, so the precise regulation of nanofluidic channels is critical for the desired membranes [11]. Ideally, the permeation characteristics of laminate membranes made from 2D materials are expected to be dominantly governed by the interlayer spacing formed between neighboring nanoflakes [30,31]. The voids from less ordered stack of nanoflakes would make the transport of molecules less controllable. The deposition rate of nanoflakes results in the formation of voids.

We made two d-MXene membranes with identical mass loading (0.3 mg/cm^2) *via* vacuum filtration using d-MXene colloidal suspension of different concentrations. The identical loading and preparation could eliminate the impact of in-plane defects and galleries structures. So the impact of voids can be confirmed. The time for preparing the membranes is greatly increased from 18 min to 285 min, as the feeding concentration diluted from 0.27 mg/mL to 0.0081 mg/mL. The longer preparation time indicates the slower deposition rate of d-MXene nanoflakes. The faster deposition rate was believed to produce relatively random packing of 2D materials, such as single layer graphene oxide, leading to the change in water permeation [32]. However, the XRD patterns of the two as-made d-MXene membranes show negligible change (Fig. 3a), suggesting the almost identical stack of nanoflakes or galleries. These films share a same interlayer distance of 1.71 nm. If the interlayer galleries is the dominantly channel for water transport, it is expected that these membranes will show the similar water permeation characteristic. Nevertheless, the membranes have

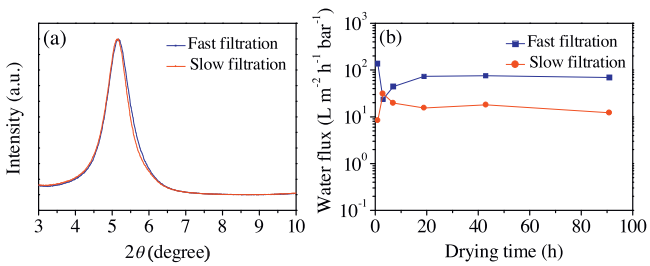

Fig. 3. (a) XRD patterns and (b) water flux of d-MXene membranes made at different filtration rates. The membranes have identical loading of 0.3 mg/cm^2.

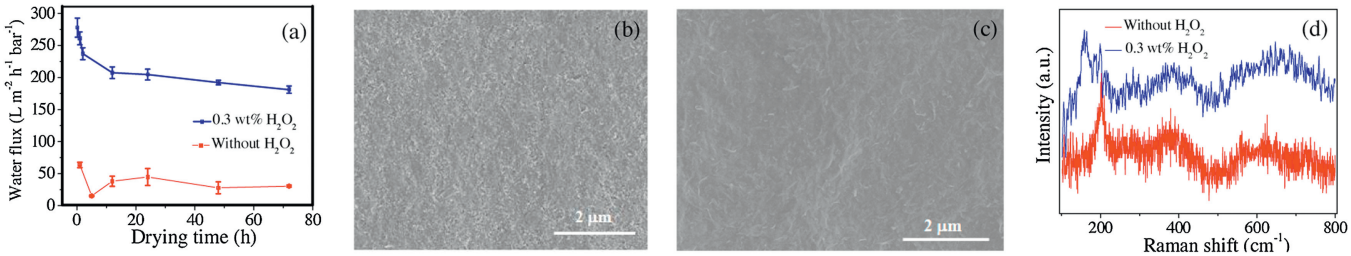

Fig. 4. (a) the impact of oxidation of d-MXene membranes on water flux. (b) SEM image of d-MXene membrane oxidized using 10 mL 0.3 wt% H_2O_2. (c) SEM image of d-MXene without oxidization. (d) Raman spectra of d-MXene membranes with and without oxidation. The loading of the d-MXene membranes were 0.3 mg/cm^2.

notably different water flux as shown in Fig. 3b. The water flux dramatically decreases as the deposition rate reduced.

The slow deposition rate produces the membrane with the smaller water flux of around 8 L m^{-2} h^{-1} bar^{-1}, while the fast rate produces the larger water flux of about 140 L m^{-2} h^{-1} bar^{-1}. These membranes also demonstrate different responses in water permeability during drying. After drying for 2 h, the fast one shows dramatically retarded water flux, while the slow one shows slight increased flux. These results suggest that there are other water channels besides interlayer galleries. The defect pores in nanoflakes should be the same as we used identical d-MXene suspension and mass loading. The formed voids are responsible for the diverse water permeation characteristics of d-MXene membranes. The voids would fill with water during water flux test. During the drying, water was removed while the capillary force leads to the compaction of the voids.

Since voids from less ordered stack, are inevitable during the build-up of laminate membranes [24]. A much severer compaction will be achieved in the membranes with more voids [24]. This explains that the faster membrane shows the most obvious decrease in water flux. It is to mention that the voids are rather localized through the entire membrane, so they are hard to observe using SEM (Fig. S5 in Supporting information).

In order to demonstrate that the voids have great impacts on the membrane performance, we used H_2O_2 to treat the d-MXene membrane. As shown in Fig. 4a, the water flux is greatly enhanced *via* filtration diluted H_2O_2 solution. The SEM images indicate that many holes developed on the d-MXene membrane after the oxidation treatment, compared with the one without oxidation (Figs. 4b and c). The holes randomly distributed, due to the voids are rather localized through the entire membrane. The Raman spectra show that the Raman bands (Fig. 4d, around 250, 400 and 600 cm^{-1}) of MXene still exist after oxidation [33]. A new peak around 150 cm^{-1} appears, corresponding to anatase TiO_2 [34]. It is well-known that MXene has limited oxidative resistance [34,35]. The voids would accommodate more H_2O_2, facilitating the oxidation and resulting in expanded channels for water transport. Oxidizing agents are inevitable in water treatment. So these voids should be avoided during membrane preparation to lessen oxidation and enhance the long-term stability of d-MXene membranes. On the other hand, the voids can be utilized as the electrolyte reservoirs and channels to improve the rate performance of energy storage devices.

Herein, we show that the water flux of the membranes assembled from d-MXene is dependent on the mass loading, drying process, deposit rate of d-MXene nanoflakes and oxidation. The interior stack structures of d-MXene membranes are similar, due to the same deposit process made by vacuum filtration. The voids from less ordered d-MXene nanoflakes, rather than the in-plane defects and interlayer galleries, play the critical role for dramatic change in water flux and can be control *via* proper processing process, such as slow deposit. The findings in this research indicate the importance of process-structure-performance relationship of d-MXene membranes, which is useful for design and assembly of desired membranes using d-MXene.

Declaration of competing interest

The authors declare that they have no known competing financial interests or personal relationships that could have appeared to influence the work reported in this paper.

Acknowledgments

This research was financially supported by the National Natural Science Foundation of China (Nos. 51606027, 51436003, 51890911), the Fundamental Research Funds for the Central Universities of China, the National Key Research and Development Program of China (Nos. 2017YFC0307300, 2016YFC0304001), the project funded by China Postdoctoral Science Foundation.

Appendix A. Supplementary data

Supplementary material related to this article can be found, in the online version, at doi:https://doi.org/10.1016/j.cclet.2019.10.037.

References

[1] J. Abraham, K.S. Vasu, C.D. Williams, et al., Nat. Nanotechnol. 12 (2017) 546–550.
[2] L. Wang, M.S.H. Boutilier, P.R. Kidambi, et al., Nat. Nanotechnol. 12 (2017) 509–522.
[3] G. Liu, W. Jin, N. Xu, Chem. Soc. Rev. 44 (2015) 5016–5030.
[4] K. Shehzad, Y. Xu, C. Gao, et al., Chem. Soc. Rev. 45 (2016) 5541–5588.
[5] X. Jiang, S. Liu, W. Liang, et al., Laser Photon. Rev. 12 (2018) 1700229.
[6] X. Jiang, W. Li, T. Hai, et al., 2D Mater. Appl. 3 (2019) 1–9.
[7] J. Liu, X. Jiang, R. Zhang, et al., Adv. Funct. Mater. 29 (2019) 1807326.
[8] C. Xing, S. Chen, X. Liang, et al., ACS Appl. Mater. Interfaces 10 (2018) 27631–27643.
[9] C. Tan, X. Cao, X. Wu, et al., Chem. Rev. 117 (2017) 6225–6331.
[10] J. Zhao, J. Zhu, R. Cao, et al., Nat. Commun. 10 (2019) 4062.
[11] H. Yan, F. Wu, Y. Xue, K. Bryan, W. Ma, P. Yu, L. Mao, Chem.-Eur. J. 25 (2019) 3969–3978.
[12] B. Anasori, M.R. Lukatskaya, Y. Gogotsi, Nat. Rev. Mater. 2 (2017) 16098.
[13] M. Naguib, V.N. Mochalin, M.W. Barsoum, Y. Gogotsi, Adv. Mater. 26 (2014) 992–1005.
[14] Z. Lu, Y.Y. W, J.J. Deng, et al., ACS Nano 13 (2019) 10535–10544.
[15] M. Ghidiu, M.R. Lukatskaya, M. Zhao, Y. Gogotsi, M.W. Barsoum, Nature 516 (2014) 78–81.
[16] B. Anasori, Y. Xie, M. Beidaghi, et al., ACS Nano 9 (2015) 9507–9516.
[17] B. Akuzum, K. Maleski, B. Anasori, et al., ACS Nano 12 (2018) 2685–2694.
[18] M. Alhabeb, K. Maleski, B. Anasori, et al., Chem. Mat. 29 (2017) 7633–7644.
[19] K. Rasool, R.P. Pandey, P.A. Rasheed, et al., Mater. Today 30 (2019) 80–102.
[20] X. Xie, C. Chen, N. Zhang, et al., Nat. Sustain. 2 (2019) 856–862.
[21] Y. Sun, S. Li, Y. Zhuang, et al., J. Membr. Sci. 591 (2019) 117350.
[22] C.E. Ren, M. Alhabeb, B.W. Byles, et al., ACS Appl. Nano Mater. 1 (2018) 3644–3652.
[23] D. McAteer, I.J. Godwin, Z. Ling, J.N. Coleman, et al., Adv. Energy Mater. 8 (2018) 1702965.
[24] V. Saraswat, R.M. Jacobberger, J.S. Ostrander, et al., ACS Nano 12 (2018) 7855–7865.
[25] Z. Wang, Q. Tu, S. Zheng, et al., Nano Lett. 17 (2017) 7289–7298.
[26] C.L. Ritt, J.R. Werber, A. Deshmukh, M. Elimelech, Environ. Sci. Technol. 53 (2019) 6214–6224.

[27] S. Zheng, Q. Tu, J.J. Urban, S. Li, B. Mi, ACS Nano 11 (2017) 6440–6450.
[28] C. Yeh, K. Raidongia, J. Shao, Q. Yang, J. Huang, Nat. Chem. 7 (2015) 166–170.
[29] C.E. Ren, K.B. Hatzell, M. Alhabeb, et al., J. Phys. Chem. Lett. 6 (2015) 4026–4031.
[30] R.R. Nair, H.A. Wu, P.N. Jayaram, I.V. Grigorieva, A.K. Geim, Science 335 (2012) 442–444.
[31] R.K. Joshi, P. Carbone, F.C. Wang, et al., Science 343 (2014) 752–754.
[32] W.L. Xu, C. Fang, F. Zhou, et al., Nano Lett. 17 (2017) 2928–2933.
[33] B. Ahmed, D.H. Anjum, M.N. Hedhili, Y. Gogotsi, H.N. Alshareef, Nanoscale 8 (2016) 7580–7587.
[34] M. Naguib, O. Mashtalir, M.R. Lukatskaya, et al., Chem. Commun. 50 (2014) 7420–7423.
[35] C.J. Zhang, S.J. Kim, M. Ghidiu, et al., Adv. Funct. Mater. 26 (2016) 4143–4151.